American Mineralogist, Volume 63, pages 947–955, 1978

Zoned plagioclase and peristerite formation in phyllites from southwestern Massachusetts

GORDON L. NORD, JR., JANE HAMMARSTROM AND E-AN ZEN

U.S. Geological Survey
Reston, Virginia 22092

Abstract

Compositionally-zoned microporphyroblasts of plagioclase are found in phyllites from southwestern Massachusetts. Rocks from the lowest metamorphic grade yield unzoned albite. At slightly higher grade, albite constitutes the core and a thin outer rim with an intervening narrow zone of An 13–17. At higher grades, plagioclase is complexly zoned in one of two patterns: either the composition drops stepwise from an oligoclase core to an albitic rim, or the composition of the core gradually increases outward from An 19 to An 24, then abruptly drops to an albite rim. All of these patterns are present in rocks at metamorphic grades below the first appearance of chloritoid and garnet. Above the garnet isograd, the zoning pattern is simple: a core of An 13 and a gradual outward increase to the maximum value of An 25.

Transmission-electron-microscopy studies of an oligoclase core, an An 9–16 intermediate zone, and an An 1–5 outer albite rim show that two sets of lamellae are present in the composition range An 2–25. In the range An 9–16, the $(1,18,\bar{1})$ set of lamellae is strong, has a periodicity of about 122A, and gives rise to satellites; the other set, $(20\bar{1})$, is weak. In the range An 22–25 both sets are very weak, and diffuse streaking is parallel to $[20\bar{1}]^*$. All areas have only a single lattice. The strong microstructures are interpreted as products of spinodal decomposition, and the weak lamellar microstructures as fluctuations in the nucleation-only zone of the peristerite solvus.

The rocks were metamorphosed probably at about 350°C and under at most a few kilometers overburden, which represents conditions considerably below the peak of the peristerite solvus. Metastable crystallization is indicated. Available data, however, do not permit an unequivocal conclusion on whether the zoned plagioclase grew during a single episode of metamorphism, or whether the albitic rim represents a second Acadian metamorphism superposed on preexisting Taconian mineral assemblages.

Introduction

The composition and "structural state" of plagioclase have been commonly used as an indicator of the geologic record in many types of petrologic and geologic problems. In detail, however, plagioclase is exceedingly complex and contains submicroscopic intergrowths and domains of distinct compositions or structural types even for samples homogeneous on an optical and microprobe scale. Subsolidus decomposition products such as intergrowths in the compositional regions of peristerite (An_2–An_{16}), Bøggild (An_{48}–An_{59}), and Huttenlocher (An_{67}–An_{90}) (Smith, 1974, p. 519) are fairly common in high-temperature igneous and metamorphic rocks. In low-grade metamorphic rocks, where plagioclase only forms with compositions in the albite–oligoclase range, the peristerite two-phase field is commonly expressed by the absence of peristerite compositions or by the presence of two coexisting plagioclases. Multiply-zoned plagioclase porphyroblasts in low-grade greenschist facies pelitic rocks from southwestern Massachusetts and adjacent areas (Zen and Hartshorn, 1966; Zen and Ratcliffe, 1971), however, contain compositional zones that are within the peristerite field (An_2–An_{16}) mantled by Ca-free albite rims. Such multiply-zoned plagioclase is present only in a relatively narrow north–northeast trending belt, coinciding with or just below the metamorphic zone where garnet makes its first appearance in rocks of suitable composition. At lower metamorphic grade, the porphyroblasts of plagioclase are nearly Ca-free albite of uniform composition, whereas at higher grades they are gradationally zoned, and the An content increases steadily outward.

This paper presents a systematic microprobe study

0003-004X/78/0910-0947$02.00

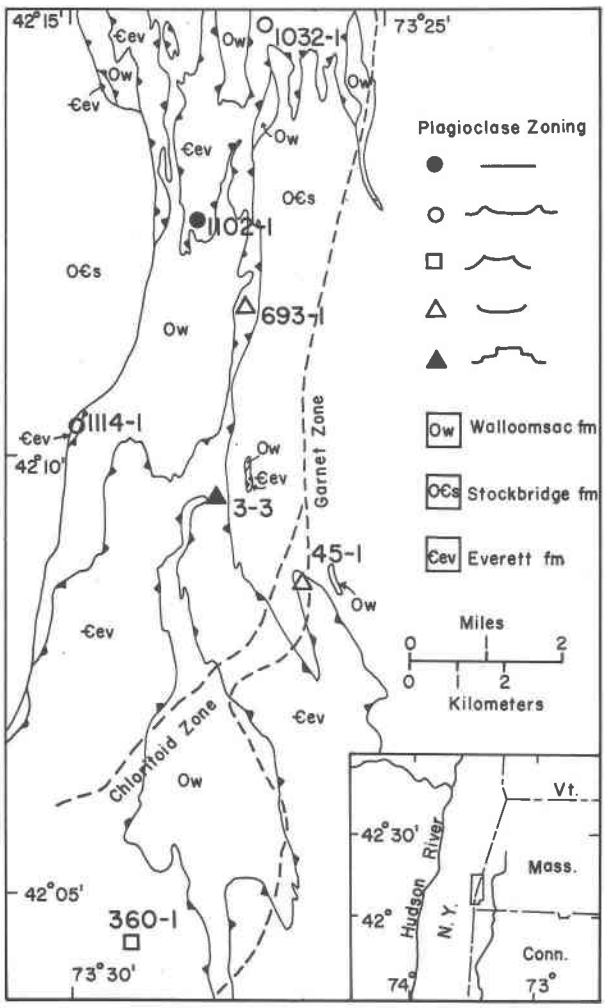

Fig. 1. Geologic map of area in southwestern Massachusetts (see inset for location), showing sample locations and their relation to the mapped isograds. The various types of plagioclase zoning discussed in the text are given different symbols on the map, and the zoning pattern is schematically shown. The symbols for 45-1 and for 693-1 are the same; however, 45-1 has an oligoclase core, and 693-1 has an albite core. Cev and Ow are the pelitic units.

of the compositional variations across the plagioclase porphyroblasts at different metamorphic grades. We present transmission electron microscopy (TEM) observations on one multiply-zoned sample and attempt to interpret the results in terms of the plagioclase subsolidus relations and the metamorphic history of the area.

Geological setting

The pelitic rocks in which the plagioclase porphyroblasts occur are part of the Taconic allochthon (Fig. 1). The rocks were emplaced during the Taconian deformation, were mildly metamorphosed, probably to the chloritoid zone, and were subsequently regionally metamorphosed again during the Acadian deformation (Zen and Hartshorn, 1966) to grades ranging from subchloritoid–subbiotite zone to kyanite–staurolite zone; the metamorphic grades increase to the SE and cut across the regional structural trend.

Interpretation of the Acadian mineral assemblages in light of experimental phase-equilibrium data suggests that rocks of the kyanite–staurolite grade, southeast of the area shown on Figure 1, recrystallized at a temperature of about 550°C and a pressure in excess of the triple point of the aluminum silicate polymorphs—at least 4 kbar or about 14 km of overburden. Yet only about 35 km to the northwest, at Becraft Mountain in New York, Silurian and Lower Devonian sedimentary rocks are unmetamorphosed and probably were not buried under more than about 1 km of stratigraphic overburden ($T \sim 50$°C). Interpolation of pressure and temperature values is uncertain. The mineral-assemblage data for the zone of complexly-zoned plagioclase (below chloritoid zone), however, suggest temperatures of about

Table 1. Representative plagioclase analyses from specimen 3-3

	3-3 TRAVERSE I Distance into crystal					
	30μ	45μ	60μ	75μ	100μ	130μ
SiO_2	67.71	67.70	65.58	66.00	64.12	63.07
Al_2O_3	20.55	20.04	21.00	21.63	23.02	24.00
CaO	0.19	0.78	2.09	2.43	3.52	4.77
K_2O	0.15	0.19	0.0	0.13	0.16	0.20
Na_2O	11.65	11.57	10.48	10.45	9.79	8.96
Σ	100.25	100.28	99.15	100.64	100.61	101.00
Si	2.955	2.958	2.902	2.884	2.813	2.764
Al	1.056	1.032	1.095	1.113	1.189	1.238
Ca	0.007	0.036	0.099	0.113	0.165	0.224
K	0.007	0.010	0.0	0.006	0.009	0.010
Na	0.985	0.979	0.898	0.885	0.833	0.760
Σ	5.010	5.015	4.994	5.001	5.009	4.996
	rim ←					→ core

Oxide weight per cents corrected for background, drift, deadtime, and matrix effects by an on-line Bence-Albee data reduction scheme (1968). Standards: calcic labradorite from Lake Co., Ore. (Stewart et al., 1966), orthoclase from the Benson Mine, St. Lawrence Co., N.Y. (Stewart and Wright, 1974) and albite from the Tiburon Peninsula, Calif. (Crawford, 1966b).

Cations calculated on the basis of 8 oxygens per formula.

Operating conditions 15 kV, .03 μA beam current for 3-3 analyses,

Each element counted for 20 secs or 20,000 counts; no Fe detected in appreciable amounts.

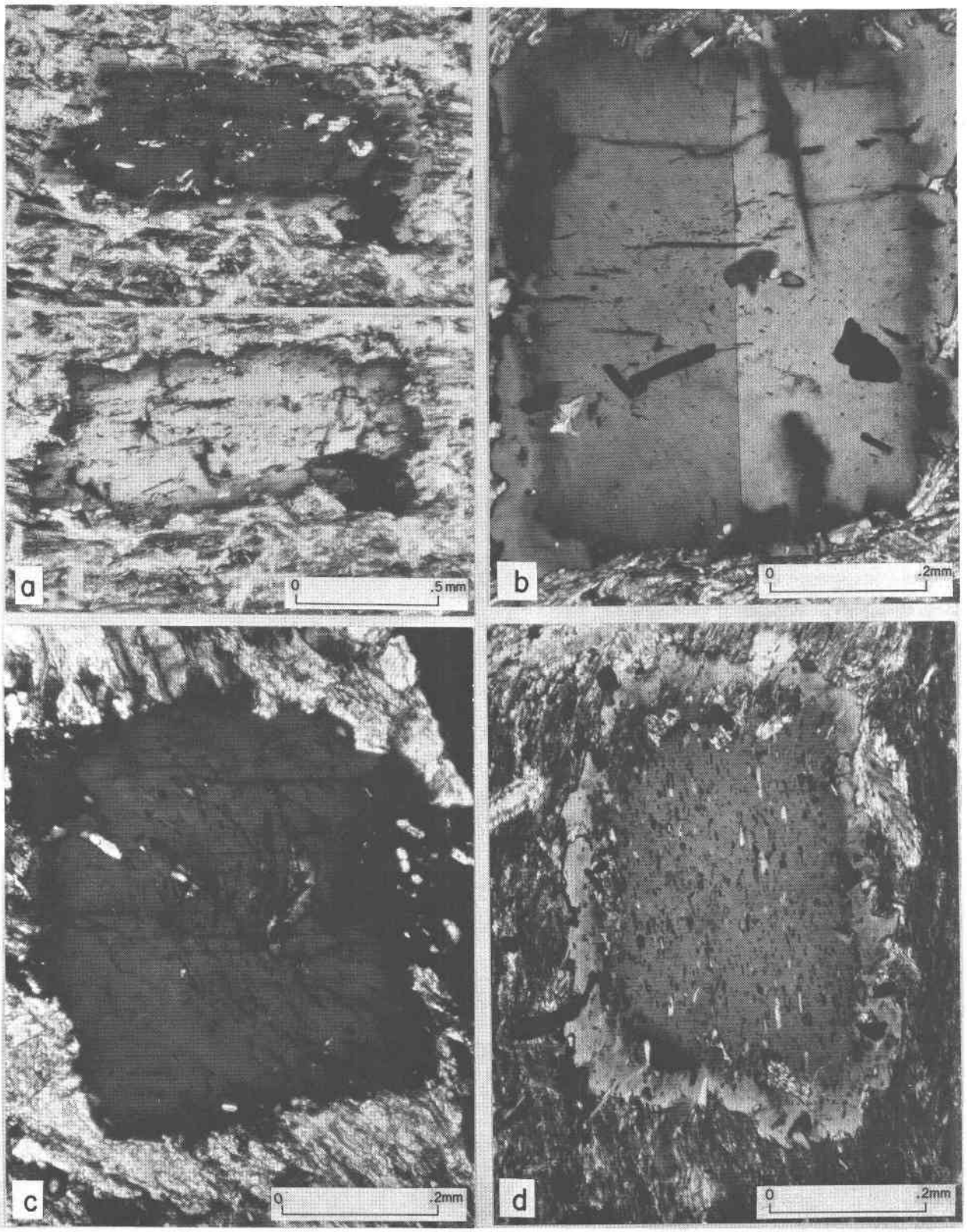

Fig. 2. Photomicrographs of plagioclase porphyroblasts, showing different modes of zoning. (a) Specimen 3-3, two views of the same crystal at slightly different extinction positions to bring out zoning features. (b) Specimen 1032-1, showing a simple twinned and zoned crystal; the core has the same composition as the rim but an intermediate zone (dark band) has a composition of An 13. (c) Specimen 693-1, showing continuous zoning from core outward with increasing An content and no albite rim. (d) Specimen 360-1, showing multiple zoning as in 3-3 but having a core lower in An content than the intermediate zone. Photographs under crossed polarizer.

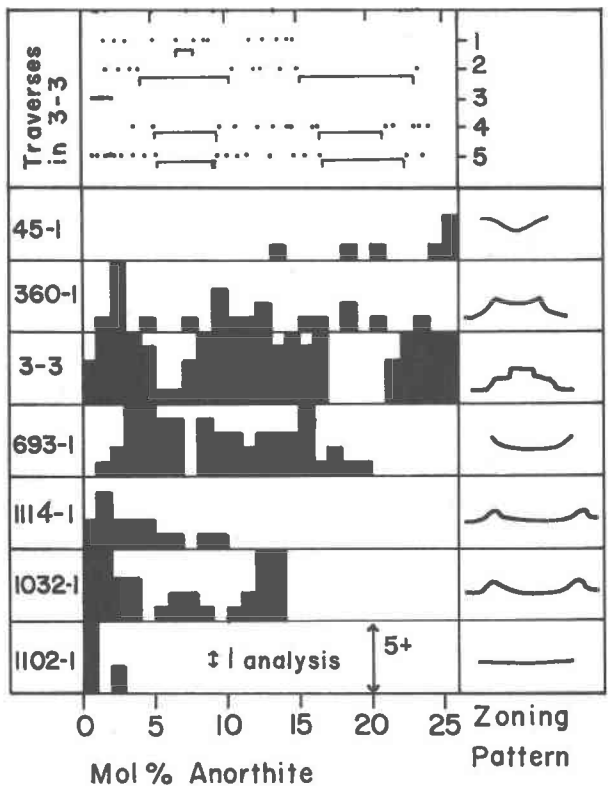

Fig. 3. Microprobe analyses of plagioclase porphyroblasts. The upper part of the figure shows compositions at points along traverses only from porphyroblasts in sample 3-3. Each dot is an individual analysis and the brackets indicate the positions of optically visible boundaries which correspond to compositional breaks in the traverse. The lower part of the figure shows histograms which relate the number of analyses to the composition of analyses from porphyroblasts in each of the seven samples. The shape of the general zoning profile for each sample is shown on the right with An content increasing upwards. Although the traverses in 3-3 in the upper part of the figure show that the positions if not the widths of the compositional gaps from porphyroblasts in a single rock are reproducible, the histograms show that the gap positions are not reproducible from sample to sample.

300–400°C at a few kilometers of overburden, compatible with a simple straight-line interpolation of the distance between Becraft Mtn. and the kyanite occurrence. The temperature estimates and the mineral assemblage both conflict with the temperature for the crest of the peristerite solvus, which was suggested by Crawford (1966a) to be well in the staurolite zone of regional metamorphism; Crawford based this suggestion on study of compositions of discrete coexisting plagioclase crystals.

The phyllites of the Everett Formation containing the plagioclase porphyroblasts are typically green and purplish-green and show few visible mineral grains in hand specimens. A conspicuous foliation and crenulated cleavage due to layers of aligned muscovite and chlorite are usually present. The porphyroblasts of plagioclase, the only feldspar phase in the rocks, are subequant to crudely elliptic in outline and are interfoliate; the long dimensions of the crystals are aligned with the foliation direction. In general each single crystal forms in a discrete area; porphyroblasts are well separated.

Reconnaissance compositional data on the multiply-zoned plagioclase porphyroblasts showed that the Na-rich oligoclase cores were continuously zoned to more Ca-rich oligoclase and then mantled with Ca-free albite. The Na- to Ca-rich zoning of the oligoclase core could be readily interpreted as a record of a normal regional prograde metamorphic event. The presence of the reversal to a Ca-free albite rim led Zen (1969) to the interpretation that the albite rim records the Acadian metamorphic event but the oligoclase core is part of a slightly higher-grade Taconian mineral assemblage. The detailed microprobe and TEM observations lead to a reevaluation of the earlier interpretation.

Optical description and microprobe analysis of the porphyroblasts

Several zoning patterns were discovered in plagioclase porphyroblasts from seven sample localities shown in Figure 1. Plagioclase compositions were determined by analysis of porphyroblasts in thin sections using an automated ARL microprobe system (Finger and Hadidiacos, 1972). Representative analyses are given in Table 1 for a traverse in sample 3-3 in terms of corrected oxide weight percent, calculated cations, and sums. Four representative porphyroblasts are shown in Figure 2, and Figure 3 provides a

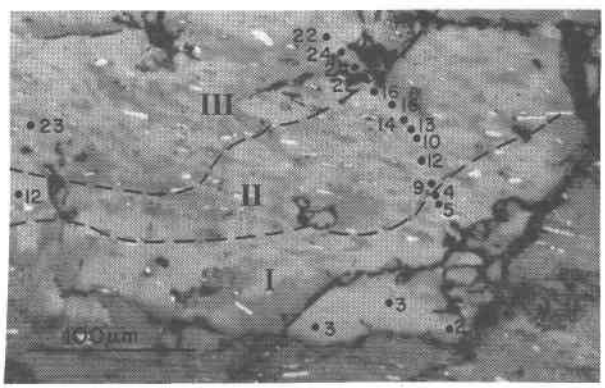

Fig. 4. Reflected-light micrograph of a part of a porphyroblast from specimen 3-3 showing two optically distinct boundaries and An content of microprobe points.

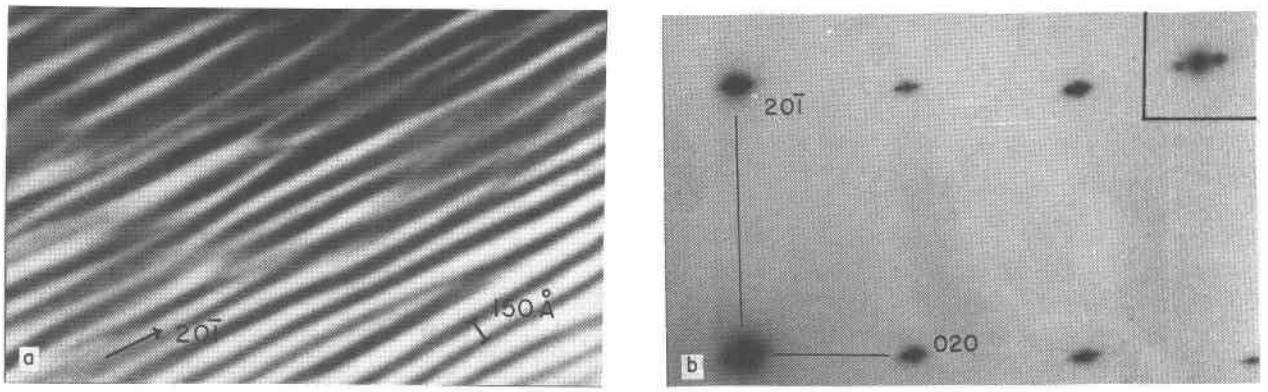

Fig 5. (a) Electron micrograph of lamellar microstructure in zone II of part of a porphyroblast from 3-3. $\vec{g} = 20\bar{1}$. (b) A selected-area electron diffraction pattern, showing satellites about each reflection. Inset is a magnified view of a reflection showing well-developed satellites. 200 kV.

summary of the microprobe data and a schematic drawing of the compositional zoning pattern across each crystal from rim to rim.

Three specimens from the lowest-grade part of the study area, 1032-1, 1102-1, and 1114-1, have albite cores and rims (Fig. 3). Specimen 1102-1 contains slightly rounded plagioclase porphyroblasts which are virtually unzoned (An 0–3). Porphyroblasts in both 1032-1 and 1114-1 have a 40- to 70-micron-wide and optically distinct band of peristerite composition, which separates the albite rim from the albite core (Fig. 2b). Maximum An content in these crystals is An 13 in the center of this band, and the An content drops off symmetrically towards the rim and core.

Plagioclase in specimen 693-1 (Fig. 2c) contains cores of albite (An 1–4). The An content increases outward from the core through peristerite compositions to a maximum of An 15–17 at the crystal margin; no discrete rim was observed. Without its albitic rim, 1032-1 would be closely similar to 693-1.

The area containing specimens 3-3, 360-1, and 45-1 marks a change from porphyroblasts having albitic core compositions to porphyroblasts with more calcic cores. Specimen 360-1 (Fig. 2d) has a core of An 18 which increases outward to a maximum of An 23 and then trails off through peristerite compositions to a distinct albite rim. It also has a well-developed rim separated from the inner parts of the crystal by a zone of alteration; the inclusions are aligned parallel to crystal length and are more concentrated in the core than in the rim. At higher grades, as in specimen 45-1, zoning is continuous, typically from An 13 at the core to An 25 at the rim.

Specimen 3-3 has been studied in detail and was also used for the TEM observations. It is a conspicuously foliated chlorite–plagioclase–muscovite–paragonite–quartz phyllite containing optically- and compositionally-zoned porphyroblasts (Fig. 2a). The boundaries of the crystals are locally complex, having jagged or embayed rims enclosing single or composite

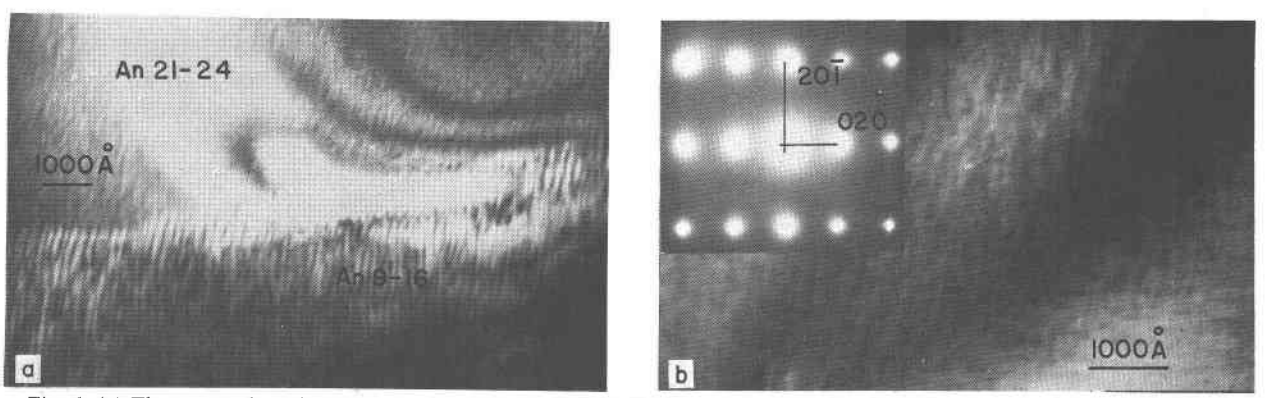

Fig. 6. (a) The coarser lamellar microstructure in zone II (Fig. 5) changes to a finer lamellar microstructure in zone III. (b) Weak lamellae in center of this core area. This fine microstructure gives rise to diffuse scattering in the diffraction pattern (inset in Fig. 6b). $\vec{g} = 20\bar{1}$, 200 kV.

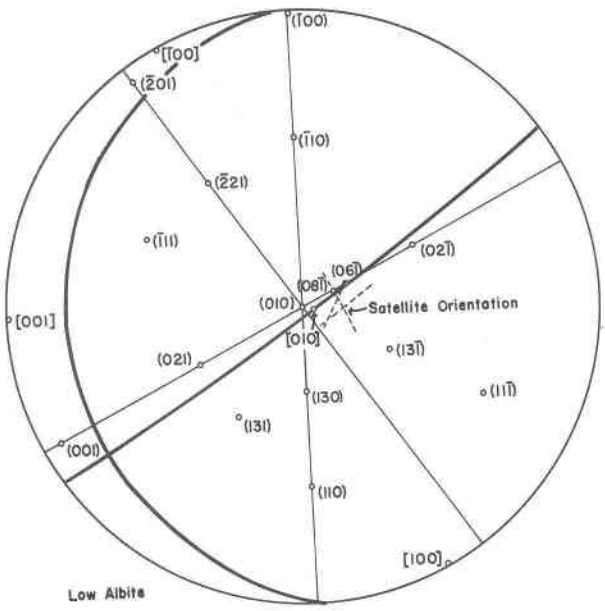

Fig. 7. Stereographic projection of low albite, showing the orientation of the satellite vector which is within the triangular area; the high-contrast lamellae near $(1,18,\bar{1})$; and the low-contrast lamellae near $(20\bar{1})$.

core crystals. Boundaries between zones are readily seen because of the different extinction positions of the zones. Rim compositions are nearly end-member albite (An 0–5). The An content increases steadily across the first optical boundary into a transition zone of composition An 9–16. Numerous point analyses, closely spaced step traverses, and backscatter images failed to reveal the existence of any abrupt compositional boundaries in the transition zone. The core of the crystal is homogeneous oligoclase, An 22–25. The core is separated from the transition zone by an optical boundary which marks a jump in composition from An 16 to 22.

In some crystals, the boundary between the oligoclase core and transition zone is partially or entirely occupied by a zone of fine-grained mixture of mica, zoisite(?), and quartz. These may be zones of alteration, and are most readily explained if they represented a zone of maximum anorthite content subsequently retrograded, and if the outer rims are due to metamorphism at a later time. Such an interpretation would be compatible with the observation of rimming of apparently embayed cores mentioned before. In favor of a single episode of crystal growth is the fact that the orientations of mineral inclusions in the crystals (especially ilmenite) seem to persist through all the zones of a given crystal, although the rims tend to have fewer inclusions, and the interface between the rim and the transition zone may show concentrations of inclusions. The oriented inclusions of the rims could have been inherited from a pre-existing mineral fabric originally in the matrix.

TEM observations

A 1-mm-long porphyroblast was chosen from sample 3-3 for the TEM study, because the compositional zones were optically distinct and the crystal was large and relatively unfractured. Three detailed microprobe traverses were made across it. The TEM samples were then prepared by ion-thinning two fragments, each containing a microprobe traverse. Figure 4 shows one fragment, with the microprobe analyses indicated, before thinning. The optically-visible boundaries marking compositional breaks divide the crystal into three zones: the rim (I), the transition zone (II), and the core (III).

In the TEM, the very albitic edge of zone I is featureless except for an occasional microtwin. In the part of zone I having the composition of peristerite (An 2–16), a very faint lamellar microstructure is visible, with a wavelength of about 100A. The electron diffraction pattern has only sharp (a) reflections.

The compositional gap between zones I and II is unrecognizable in the electron microscope; the only change is a continued gradual increase in black–white contrast of the lamellar microstructure. Once in the composition range of zone II, however, the lamellar microstructure is easily imaged (Fig. 5a), and appears to be developed evenly across this zone. The lamella split and recombine, exhibiting a connectiveness.

The contrast of the lamellae is strong for operating

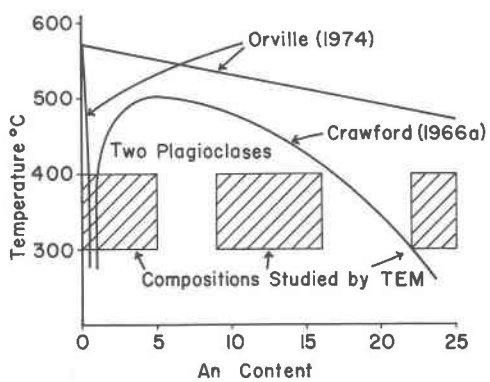

Fig. 8. A phase diagram showing the peristerite solvus of Crawford (1966a) and two-phase field of Orville (1974). The 3-3 porphyroblast compositions studied in TEM are shown between 300°C and 400°C, the estimated temperature of crystallization.

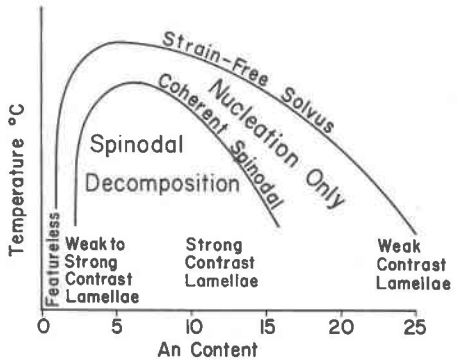

Fig. 9. The strain-free solvus and estimated coherent spinodal are shown with the TEM observations from the various portions of porphyroblast 3-3. Spinodal decomposition can occur only under the spinodal curve whereas nucleation can occur anywhere under the strain-free solvus. Thus both mechanisms compete within the coherent spinodal.

$\vec{\mathbf{g}}$ vectors containing components in the plane of the lamellae ($20\bar{1}$, $02\bar{1}$, 001) and weak for those vectors containing components normal to the plane of the lamellae (020) (see also McLaren, 1974, and Nord *et al.*, 1974). In addition, when $\vec{\mathbf{g}}$ = 020 and the strong set of lamellae visible in Figure 5a is out of contrast, a faint set of lamellae normal to the strong set is visible.

The selected-area diffraction pattern for this area (Fig. 5b) shows that the lamellae have a high degree of periodicity, because satellite reflections are found about all the main reflections. The average lamellae wavelength can be calculated from the pattern by dividing the satellite-to-main spot spacing into the appropriate camera constant K. The average real-space spacing is 122A, although a diffuse streak connects the satellites and even extends slightly beyond, indicating a range of wavelengths. In all diffraction patterns taken of the modulated structures, all main reflections were sharp and no splitting was observed. This is surprising because γ^* is the reciprocal lattice parameter that undergoes the greatest change between the exsolved phases in peristerite (1.7° between An 0 and An 25, Ribbe, 1960); even in a^*b^* diffraction patterns, only single diffraction spots were present from all three zones. Satellites were found only in zone II.

The compositional break between zones II and III is manifested as an abrupt change in lamella contrast from relatively strong contrast in zone II to weak contrast in zone III (Fig. 6a). The size and orientation of the lamellae appear constant. Within zone III, weak lamellae can be observed even at the center of the core area (Fig. 6b). Diffuse scattering seen in Figure 6b is parallel to the row $[20\bar{1}]^*$ in diffraction patterns from zone III. Type (e) reflections characteristic of intermediate plagioclase would, if present, occupy the position midway between the $20\bar{1}$ reflections [$20\bar{1}$ would be indexed $20\bar{2}$ for the 14A cell and (b) reflections would be $10\bar{1}$, $30\bar{3}$, *etc.*].

The orientation of the two sets of lamellae, one strong and one weak, is shown in Figure 7 in a stereographic projection of the crystallographic axes of low albite. Many zone-axis patterns were used for the analysis; three which nearly contain the vector connecting the satellites, ⟨001⟩, ⟨100⟩, and ⟨102⟩, are plotted. The satellite vector was located at the intersection of great circles containing the zone normal and the vector trace. The satellite vector falls 6° from ($08\bar{1}$) (c = 7A) to near ($1,18,\bar{1}$) plotted as a heavy great circle. The orientation of the weak lamellae near ($20\bar{1}$) was determined by trace analysis from the image plates, as no streaking from this lamellar set was in the diffraction pattern.

Discussion and conclusions

Peristerite phase relations

The peristerite two-phase field (recently reviewed by Smith, 1975) has been described as either a solvus or as a two-phase binary "loop." Both types of phase relations are shown in Figure 8. The solvus is asymmetrical; Crawford (1966a) estimated the low-temperature endmembers from a study of coexisting metamorphic plagioclases to be about An_1 and An_{24}. She placed the crest of the solvus between the almandine and staurolite isograds at 450°–500°C. More recent data on staurolite stability suggest that the staurolite isograd should be placed at least at 550°C (Thompson, 1976), raising the crest nearer to the high albite–low albite transition (575–625°C, McConnell and McKie, 1960). In contrast to the solvus model, a two-phase field consisting of low albite and high- to intermediate-albite solid solution is preferred by Smith (1972) and Orville (1974). Orville (1974) rejected a solvus, on the basis of experimentally-determined ideal solution behavior which occurred over the range An_0 to An_{50-55} at 700°C (Orville, 1972) and at 600°C (Orville, 1974).

The maximum temperature of crystallization of the porphyroblasts is estimated to be between 300°C and 400°C, as discussed previously, and this is indicated in Figure 8 by areas representing the compositions found in the porphyroblast 3-3, studied by TEM. The compositional breaks, however, have no significance, since the total compositions represented by all the

analysed porphyroblasts from all the samples competely span the range An_0 to An_{25} (Fig. 3). The breaks probably represent polyphase metamorphism or local changes in growth rate or reacting phases.

The homogeneous distribution, diffuse interfaces, and connective and wavelike morphology of the peristerite lamellae, as well as the formation of satellites about the main reflections in the strong contrast lamellae, suggest that the exsolution mechanism is spinodal decomposition. This conclusion is consistent with those of previous authors who have studied peristerite microstructures (Christie, 1968; Weber, 1972; Lorimer *et al.*, 1974). It should be pointed out, however, that the spinodal decomposition mechanism can only be proven by observing the progress of decomposition with time (Laughlin and Cahn, 1975; Yund, 1975b). The peristerite microstructure, therefore, could possibly have formed by homogenous nucleation and growth, but this is unlikely, in view of the difficulty of forming a critical nucleus in feldspars, especially at low temperatures (Yund, p. Y-35, 1975b), contrasted with the relative ease of spinodal decomposition, which requires no nucleation.

Unmixing in the two-phase field of the binary "loop" model can proceed only by a nucleation and growth mechanism, since the free energy curves for the two phases are discrete, and therefore spinodal decomposition is not possible (Champness and Lorimer, p. 175, 1976). Nucleation and growth, as well as spinodal decomposition, is possible in the solvus model.

Peristerite microstructure

The types of microstructures are summarized in Figure 9 on a phase diagram showing an asymmetric strain-free solvus and an asymmetric coherent spinodal curve (Christie, 1968) (see Yund, 1975a, for a detailed discussion of the curves). In the region An_{9-16} of our sample, compositional differences exist between the coherent lamellae, as indicated by the strong image contrast obtained using operating vectors for which the structure factor difference between albite and oligoclase is large [*i.e.*, for $\vec{g} = 02\bar{1}$, Fc(albite) = 0, Fc(oligoclase) = 20]. This area lies within the coherent spinodal.

Spinodal theory predicts a critical wavelength λc that is amplified during decomposition while all other wavelengths decay (Cahn, 1968). Once the decomposition is complete, the lamellae will coarsen and other waveforms will grow at the expense of λc, eliminating the sine waveform and periodic quality of the original microstructure. We suggest that the sharp satellites in the An_{9-16} region and small ~122A wavelength of the lamellae indicate that the microstructure has not coarsened to any appreciable extent. Therefore, λc is ~120A for a composition An_{9-16} at an undercooling of 100 to 200°C (Cahn, 1968).

Crosshatched lamellar microstructures which exhibited only weak contrast were also present outside the estimated spinodal curve in the An_{22-25} core (Fig. 7). McLaren (1974) found similar weak microstructures in both An_{23} and An_{26}. Although the wavelengths are similar to those in the An_{9-16} region, no satellite is present and the contrast is weak. We suggest that this microstructure is in the nucleation-only field and consists of minor fluctuations (1–2 mole percent An) in composition or structure of variable wavelength. These compositional fluctuations are the precursors to decomposition; they can amplify in the spinodal field about λc but can only decay in the nucleation-only field. The diffuse scattering in the diffraction pattern from this region may represent an attempt to form the intermediate plagioclase superlattice structure. The two sets of lamellae found in the porphyroblasts lie very close to the predicted positions of strain energy minima calculated by Willaime and Brown (1974).

Geologic inferences

Our data do not permit us to decide whether the zoning pattern of the plagioclase is the product of a single or two discrete episodes of regional metamorphism. Because the TEM observations show that the continuous microstructure is superimposed across the already-formed core–rim boundary, the data are compatible with either hypothesis for the formation of the entire porphyroblasts. In any event, however, the various rimmed porphyroblasts indicate a complexity in spatial and sequential arrangment of metamorphism not revealed by conventional microscopic petrography.

The rocks were metamorphosed probably at temperatures no higher than about 350°C and under at most a few kilometers of overburden. These conditions are considerably below estimates of the peristerite solvus (~550°C). The areas of peristerite composition therefore crystallized metastably, and those compositions within the coherent spinodal subsequently exsolved by spinodal decomposition. The low temperature of formation apparently suppressed coarsening of the microstructure and therefore preserved the high degree of lamellar periodicity.

Acknowledgments

We thank Peter T. Lyttle, Paul H. Ribbe, Richard A. Robie, and Malcolm Ross for reviewing the manuscript and giving us helpful suggestions. We also thank Lovell Wiggins for assistance with the microprobe.

References

Bence, A. E. and A. L. Albee (1968) Empirical correction factors for the electron microanalysis of silicates and oxides. *J. Geol., 76,* 382–403.

Cahn, J. W. (1968) Spinodal decomposition. *Trans. AIME, 242,* 166–180.

Champness, P. E. and G. W. Lorimer (1976) Exsolution in silicates. In H.-R. Wenk, Ed., *Electron Microscopy in Mineralogy,* p. 174–204. Springer-Verlag, New York.

Christie, O. H. J. (1968) Spinodal precipitation in silicates. I. Introductory application to exsolution in feldspar. *Lithos, 1,* 187–192.

Crawford, M. L. (1966a) Composition of plagioclase and associated minerals in some schists from Vermont, U.S.A., and South Westland, New Zealand, with inferences about the peristerite solvus. *Contrib. Mineral. Petrol., 13,* 269–294.

——— (1966b) Optical properties of metamorphic albite. *Am. Mineral., 51,* 523–524.

Finger, L. W. and C. G. Hadidiacos (1972) Electron microprobe automation. *Carnegie Inst. Wash. Year Book, 71,* 598–600.

Laughlin, D. E. and J. W. Cahn (1975) Spinodal decomposition in age hardening copper–titanium alloys. *Acta Metallurgica, 23,* 329–339.

Lorimer, G. W., H.-U. Nissen and P. E. Champness (1974) High voltage electron microscopy of a deformed plagioclase from an Alpine gneiss. *Schweiz. Mineral. Petrogr. Mitt., 54,* 707–715.

McConnell, J. D. C. and D. McKie (1960) The kinetics of the ordering process in triclinic $NaAlSi_3O_8$. *Mineral. Mag., 32,* 436–454.

McLaren, A. C. (1974) Transmission electron microscopy of the feldspars. In W. S. MacKenzie and J. Zussman, Eds., *The Feldspars,* p. 378–423. Manchester University Press, Manchester, England.

Nord, G. L., Jr., A. H. Heuer and J. S. Lally (1974) Transmission electron microscopy of substructures in Stillwater bytownite. In W. S. MacKenzie and J. Zussman, Eds., *The Feldspars,* p. 522–535. Manchester University Press, Manchester, England.

Orville, P. M. (1972) Plagioclase cation exchange equilibria with aqueous chloride solution: results at 700°C and 2000 bars in the presence of quartz. *Am. J. Sci., 272,* 234–272.

——— (1974) The peristerite gap as an equilibrium between ordered albite and disordered plagioclase solid solution. *Bull. Soc. fr. Mineral. Cristallogr., 97,* 386–392.

Ribbe, P. H. (1960) An X-ray and optical investigation of peristerite plagioclases. *Am. Mineral., 45,* 626–644.

Smith, J. V. (1972) Critical review of synthesis and occurrence of plagioclase feldspars and a possible phase diagram. *J. Geol., 80,* 505–525.

——— (1974) *Feldspar Mineralogy, Vol. 2.* Springer-Verlag, New York.

——— (1975) Phase equilibria of plagioclase. In P. H. Ribbe, Ed., *Feldspar Mineralogy.* Mineral. Soc. Am. Short Course Notes, 2.

Stewart, D. B., G. W. Walker, T. L. Wright and J. J. Fahey (1966) Physical properties of calcic labradorite from Lake County, Oregon. *Am. Mineral., 51,* 177–197.

——— and T. L. Wright (1974) Al/Si order and symmetry of natural alkali feldspars and the relationship of strained cell parameters to bulk composition. *Bull. Soc. fr. Mineral. Cristallogr., 97,* 356–377.

Thompson, A. B. (1976) Mineral reactions in pelitic rocks: II. Calculation of some *P–T–X* (Fe–Mg) phase relations. *Am. J. Sci., 276,* 425–454.

Weber, L. (1972) Das Entmischungsverhalten der Peristerite. *Schweiz. Mineral. Petrogr. Mitt., 52,* 349–372.

Willaime, C. and W. L. Brown (1974) A coherent elastic model for the determination of the orientation of exsolution boundaries: application to the feldspars. *Acta Crystallogr., A30,* 316–331.

Yund, R. A. (1975a) Subsolidus phase relations in the alkali feldspars with emphasis on coherent phases. In P. H. Ribbe, Ed., *Feldspar Mineralogy.* Mineral. Soc. Am. Short Course Notes, 2.

——— (1975b) Microstructure, kinetics and mechanisms of alkali feldspar exsolution. In P. H. Ribbe, Ed., *Feldspar Mineralogy.* Mineral. Soc. Am. Short Course Notes, 2.

Zen, E-an (1969) Petrographic evidence for polymetamorphism in the western part of the northern Appalachians and a possible regional chronology (abstr.). *Geol. Soc. Am. Abstracts with Programs for 1969,* 297–299.

——— and J. H. Hartshorn (1966) Geologic map of the Bashbish Falls quadrangle, Massachusetts, Connecticut, and New York. *U.S. Geol. Surv. Geol. Quad. Map, GQ-507.*

——— and N. M. Ratcliffe (1971) Bedrock geologic map of the Egremont quadrangle and adjacent areas, Berkshire County, Massachusetts, and Columbia County, New York. *U.S. Geol. Surv. Misc. Geol. Invest. Map I-628.*

Manuscript received, March 31, 1978; accepted for publication, May 25, 1978.